frontiers | Frontiers in Immunology

TYPE Original Research
PUBLISHED 14 November 2022
DOI 10.3389/fimmu.2022.1027449

OPEN ACCESS

EDITED BY
Guru P. Sonpavde,
Dana–Farber Cancer Institute,
United States

REVIEWED BY
Fabio Grizzi,
Humanitas Research Hospital, Italy
Emil Bulatov,
Kazan Federal University, Russia

*CORRESPONDENCE
Jing Quan
quanjing1993@hotmail.com
Feng Liu
liufeng2408@sina.com

†These authors have contributed equally to this work

SPECIALTY SECTION
This article was submitted to Cancer Immunity and Immunotherapy, a section of the journal Frontiers in Immunology

RECEIVED 25 August 2022
ACCEPTED 21 October 2022
PUBLISHED 14 November 2022

CITATION
Bai Y, Zhang Q, Liu F and Quan J (2022) A novel cuproptosis-related lncRNA signature predicts the prognosis and immune landscape in bladder cancer.
Front. Immunol. 13:1027449.
doi: 10.3389/fimmu.2022.1027449

A novel cuproptosis-related lncRNA signature predicts the prognosis and immune landscape in bladder cancer

Yuchen Bai†, Qi Zhang†, Feng Liu* and Jing Quan*

Urology and Nephrology Center, Department of Urology, Zhejiang Provincial People's Hospital, Affiliated People's Hospital, Hangzhou Medical College, Hangzhou, China

Background: Bladder cancer (BLCA) is one of the deadliest diseases, with over 550,000 new cases and 170,000 deaths globally every year. Cuproptosis is a copper-triggered programmed cell death and is associated with the prognosis and immune response of various cancers. Long non-coding RNA (lncRNA) could serve as a prognostic biomarker and is involved in the progression of BLCA.

Methods: The gene expression profile of cuproptosis-related lncRNAs was analyzed by using data from The Cancer Genome Atlas. Cox regression analysis and least absolute shrinkage and selection operator analysis were performed to construct a cuproptosis-related lncRNA prognostic signature. The predictive performance of this signature was verified by ROC curves and a nomogram. We also explored the difference in immune-related activity, tumor mutation burden (TMB), tumor immune dysfunction and exclusion (TIDE), and drug sensitivity between the high- and low-risk groups.

Results: We successfully constructed a cuproptosis-related lncRNA prognostic signature for BLCA including eight lncRNAs (RNF139-AS1, LINC00996, NR2F2-AS1, AL590428.1, SEC24B-AS1, AC006566.1, UBE2Q1-AS1, and AL021978.1). Multivariate Cox analysis suggested that age, clinical stage, and risk score were the independent risk factors for predicting prognosis of BLCA. Further analysis revealed that this signature not only had higher diagnostic efficiency compared to other clinical features but also had a good performance in predicting the 1-year, 3-year, and 5-year overall survival rate in BLCA. Notably, BLCA patients with a low risk score seemed to be associated with an inflamed tumor immune

microenvironment and had a higher TMB level than those with a high risk score. In addition, patients with a high risk score had a higher TIDE score and a higher half maximal inhibitory concentration value of many therapeutic drugs than those with a low risk score.

Conclusion: We identified a novel cuproptosis-related lncRNA signature that could predict the prognosis and immune landscape of BLCA.

KEYWORDS

cuproptosis, lncRNA, prognosis, immune, BLCA

Introduction

Bladder cancer (BLCA) is one of the deadliest diseases, with over 550,000 new cases and 170,000 deaths globally every year (1, 2). Despite certain pathogenic factors for the development of BLCA, including advanced age and cigarette smoking, the precise mechanism was not clear yet (3). In the past 30 years, the treatment of BLCA has evolved from surgery to a multidisciplinary approach including surgery, chemoradiotherapy, and immunotherapy (4, 5). However, the prognosis of patients with muscle-invasive BLCA was less favorable, and the 5-year survival rate was less than 50% (6). Moreover, BLCA is prone to distant metastasis when it invaded the sarcolemma (7). Until now, there is no ideal prognostic marker or signature for predicting prognosis of BLCA.

Cuproptosis is a copper-triggered programmed cell death (8). Copper is a fundamental trace element in many biological processes. Excess copper contributed to the aggregation of lipoylated dihydrolipoamide S-acetyltransferase intracellularly, leading to proteotoxic stress and cuproptosis (9). Emerging lines of evidence suggested that copper level could affect the oncogenesis and progression of cancer (10). Moreover, cuproptosis-related signature could predict the prognosis and immune response in various types of cancers, including renal cell carcinoma (11), hepatocellular carcinoma (12), and melanoma (13).

Long non-coding RNAs (lncRNAs), a series of RNA molecules with a transcript length of more than 200 nt, could regulate gene expression *via* interacting with protein, RNA, and DNA (14). Accumulating studies reported that lncRNA could serve as prognostic biomarker and be involved in the progression of BLCA. An m6A-related lncRNA signature could predict prognosis and immune landscape in BLCA (15). Moreover, lncRNA LNMAT2 could promote lymphatic metastasis in BLCA (16). As far as we know, the prognostic value of cuproptosis-related lncRNAs and their correlation with immune landscape in BLCA had not been fully elucidated. In this study, we aimed to develop a novel cuproptosis-related lncRNA signature to predict the prognosis and immune landscape of BLCA.

Materials and methods

Data extraction and processing

The workflow of the current study is shown in Figure 1. The transcriptomic data and clinical features of BLCA patients were downloaded from The Cancer Genome Atlas database (TCGA, https://portal.gdc.cancer.gov/), including 409 tumor samples and 19 normal samples. Strawberry Perl (version 5.30.0.1-64bit, https://strawberryperl.com/) was used to extract the useful information, such as the fragment per kilobase million format (FPKM) and the complete pathological information of each clinical sample. Then, Perl programming language was applied to distinguish mRNA and lncRNA. Moreover, simple nucleotide variation (SNV) data and masked somatic mutation data were also downloaded from the TCGA database, and used to calculate the mutational burden of BLCA. The cuproptosis-related genes were collected from the available online literatures, including NFE2L2, NLRP3, ATP7A, ATP7B, SLC31A1, FDX1, LIAS, LIPT1, LIPT2, DLD, DLAT, PDHA1, PDHB, MTF1, GLS, CDKN2A, DBT, GCSH, and DLST (17–21).

Screening the differentially expressed cuproptosis-related lncRNAs

Limma package by R language (version 4.2.1, https://www.r-project.org/) was used to screen the differentially expressed genes. Then, Pearson's correlation analysis was performed to assess the association between cuproptosis-related genes and cuproptosis-related lncRNAs. When Pearson's correlation coefficient was greater than 0.4 and p-value was less than

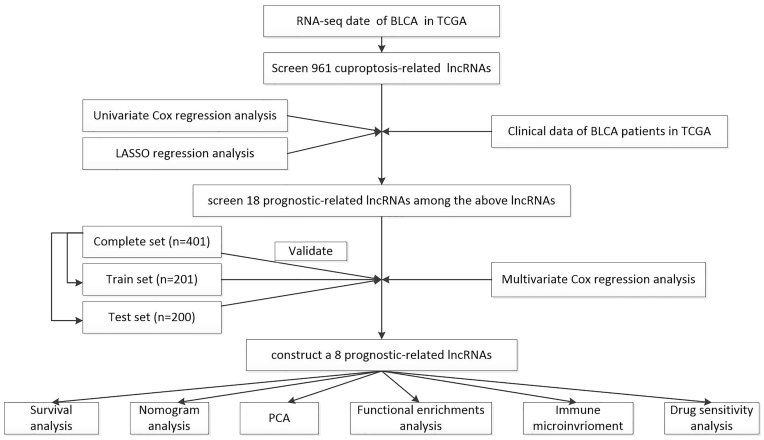

FIGURE 1
The workflow of the current study.

0.001, these lncRNAs were considered to be related to cuproptosis and were statistically significant. The above result was visualized by using a Sankey diagram.

Constructing a novel prognostic risk model of cuproptosis-related lncRNAs

By combining candidate lncRNAs with clinical data, the information about the expression and survival status of each lncRNA in clinical samples was obtained. Then, using the R package, the BLCA dataset downloaded from the TCGA database was randomly divided into two groups: train group and test group. The train group was used to construct the cuproptosis-related lncRNA signature, and the test group was used to validate the signature. Finally, the risk model was applied in the complete group. To further verify the prognosis-related lncRNAs among those candidate lncRNAs, univariate Cox regression analysis was performed ($p < 0.05$).

Next, least absolute shrinkage and selection operator (LASSO) regression analysis and lambda spectra are used to screen prognosis-related lncRNAs in order to prevent overfitting when constructing a prognostic risk model. Our research modified the LASSO regression analysis as follows: Run 1,000 cycles, and set 1,000 random stimuli in each cycle. In the next step, record the frequency of each pair of LASSO regression models that are repeated 1,000 times, and select the pairs with a frequency of more than 100 times to perform multivariate Cox proportional hazard regression analysis and build the model. Then, calculate the AUC values of these models. When the AUC value reaches the maximum value, it indicates that the model is the best candidate model. In this study, the risk score is obtained by the following formula: Risk Score= $\sum$ inCoef(i)*Expr(i). In the above formula, inCoef(i) means the corresponding correlation coefficient of each lncRNA, while Expr(i) represents the corresponding standardized expression level of each lncRNA. After classifying BLCA samples in a low- or a high-risk subgroup in the training set, the test set, or the entire TCGA BLCA dataset, we then drew the overall survival (OS) and progression-free survival (PFS) of BLCA patients with the Kaplan–Meier (KM) method using the "survival" R package. The association between risk and clinical characteristics was analyzed with chi-square test. In order to analyze the accuracy of this risk model in the prognosis of BLCA, we also generated ROC curves and the consistency index (C-index) with "glmnet" and "timeROC" packages. Considering risk score and clinical characteristics, we then drew a nomogram and a calibration curve to evaluate the predictive power of a prognostic module in 1-, 3-, and 5-year OS using the "rms" package with the Hosmer–Lemeshow test.

Principal components analysis and functional enrichments analysis

In order to visualize the expression patterns of cuproptosis-related lncRNAs in BLCA samples, principal components analysis (PCA) was conducted with the "scatterplot3d" package. After screening differential genes between the low- and high-risk groups, we performed Gene Ontology (GO) and KEGG pathways analysis with the "clusterProfiler" and "enrichplot" packages with FDR < 0.05 as threshold value. GO components included biological process (BP), cellular component (CC), and molecular function (MF).

Immune infiltration

In order to evaluate the difference in immune infiltration between the high- and the low-risk group, we performed GSVA using the "reshape2" package and the "GSEABase" package. Furthermore, the methods such as XCELL (22), TIMER (23), QUANTISEQ (24), MCPCOUNTER (25), EPIC (26), CIBERSORT (27), and CIBERSORT-ABS (28) were applied to explore the relationship between risk scores and tumor-infiltrating immune cells. The Wilcoxon signed-rank test was used to analyze the differences in the content of immune infiltrated cells explored by the above methods between the high-risk and the low-risk group. Moreover, the relationship between risk scores and immune infiltrated cells was displayed by Spearman correlation analysis. A lollipop diagram was used to display the above results. The operation was performed using the ggplot2 package for R.

Tumor mutation burden and drug sensitivity analysis

The somatic mutation data were also obtained from the TCGA website. The TMB oncoplot in the high-risk and low-risk groups was drawn with the "maftools" package. The KM method was used to draw the OS curve in the high and low TMB score group. After obtaining the tumor immune dysfunction and exclusion (TIDE) score from their website (http://tide.dfci.harvard.edu), we then analyzed the difference of TIDE score in the low- and high-risk groups of BLCA samples. Moreover, half maximal inhibitory concentration (IC_{50}) values of different drugs in the high- and low-risk groups of BLCA samples were calculated with the "pRRophetic" R package.

Results

Defining the cuproptosis-related lncRNAs with prognostic significance

As shown in Figure 2A, a total of 961 cuproptosis-related lncRNAs were identified in BLCA (|Pearson R| > 0.4 and p < 0.001). Based on these 961 lncRNAs, we performed univariate Cox analysis to identify these lncRNAs with prognostic significance. As a result, a total of 18 prognostic cuproptosis-related lncRNAs, namely, AC004466.3, AC125494.1, AC124248.2, RNF139-AS1, LINC00996, NR2F2-AS1, AL590428.1, AC073534.2, AL163952.1, SEC24B-AS1, LINC00426, BX546450.2, AL590133.1, AC006566.1, GS1-594A7.3, UBE2Q1-AS1, AL021978.1, and AL137779.1, were obtained (Figure 2B, p < 0.05).

Development of a cuproptosis-related lncRNA prognostic signature

Based on the above 18 prognostic cuproptosis-related lncRNAs, we then performed a LASSO Cox regression analysis to construct a cuproptosis-related lncRNA prognostic signature in BLCA. As a result, this multi-Cox proportional risk model consisted of eight cuproptosis-related lncRNAs. Figures 2C, D revealed the coefficient and partial likelihood deviance of the multi-Cox proportional risk model. The correlation between cuproptosis-related genes and eight prognostic lncRNAs are shown in Figure 2E. The risk score of each BLCA case was calculated with the multivariate Cox regression formula: RNF139-AS1× (−0.478075619) + LINC00996× (−0.683046976) + NR2F2-AS1× (1.081783641) + AL590428.1× (1.423045357) + SEC24B-AS1× (−1.138326443) + AC006566.1× (−0.296157307) + UBE2Q1-AS1× (−0.360369461) + AL021978.1× (−0.26913395). TCGA BLCA cases were clustered in the high- and low-risk groups with a medium risk score as the cutoff value in the train set, the test set, and the complete set. The risk core, survival status, and gene expression of the train set, the test set, and the complete set are shown in Figures 3A–I. As expected, significant poor OS was obtained in BLCA cases with a high risk score in the train set (Figure 3J, p < 0.001), the test set (Figure 3K, p = 0.04), and the complete set (Figure 3L, p < 0.001). Unfortunately, although this model was a good predictor of PFS in BLCA patients in both train and complete groups (Figures 3M, O), it was not significant in the test group (Figure 3N). Further univariate and multivariate Cox analysis suggested that age, clinical stage, and risk score were the independent risk factors for prognosis of BLCA (Figures 4A, B).

Evaluation of the predictive power of the cuproptosis-related lncRNA prognostic signature

Compared with the AUC of the ROC curve about age, sex, tumor grade, and clinical stage, the AUC of the ROC curve of risk score was the highest (Figure 4C). The AUC was 0.692, 0.692, and 0.721 for the 1-, 3-, and 5-year ROCs, respectively (Figure 4D). The 10-year C-index in the cuproptosis-related lncRNA prognostic signature was also higher than other clinical features (Figure 4E). These lines of evidence revealed that the cuproptosis-related lncRNA prognostic signature had a better predictive power compared to other clinicopathological characteristics. In order to predict the survival possibility of BLCA patients at 1, 3, and 5 years, we also constructed a nomogram considering clinical characteristics and risk scores, and the results are shown in Figures 5A, B. As expected, the calibration curves showed good agreement between the nomogram and the predicted results in 1-, 3-, and 5-year OS (Figure 5B). Moreover, we also verified this

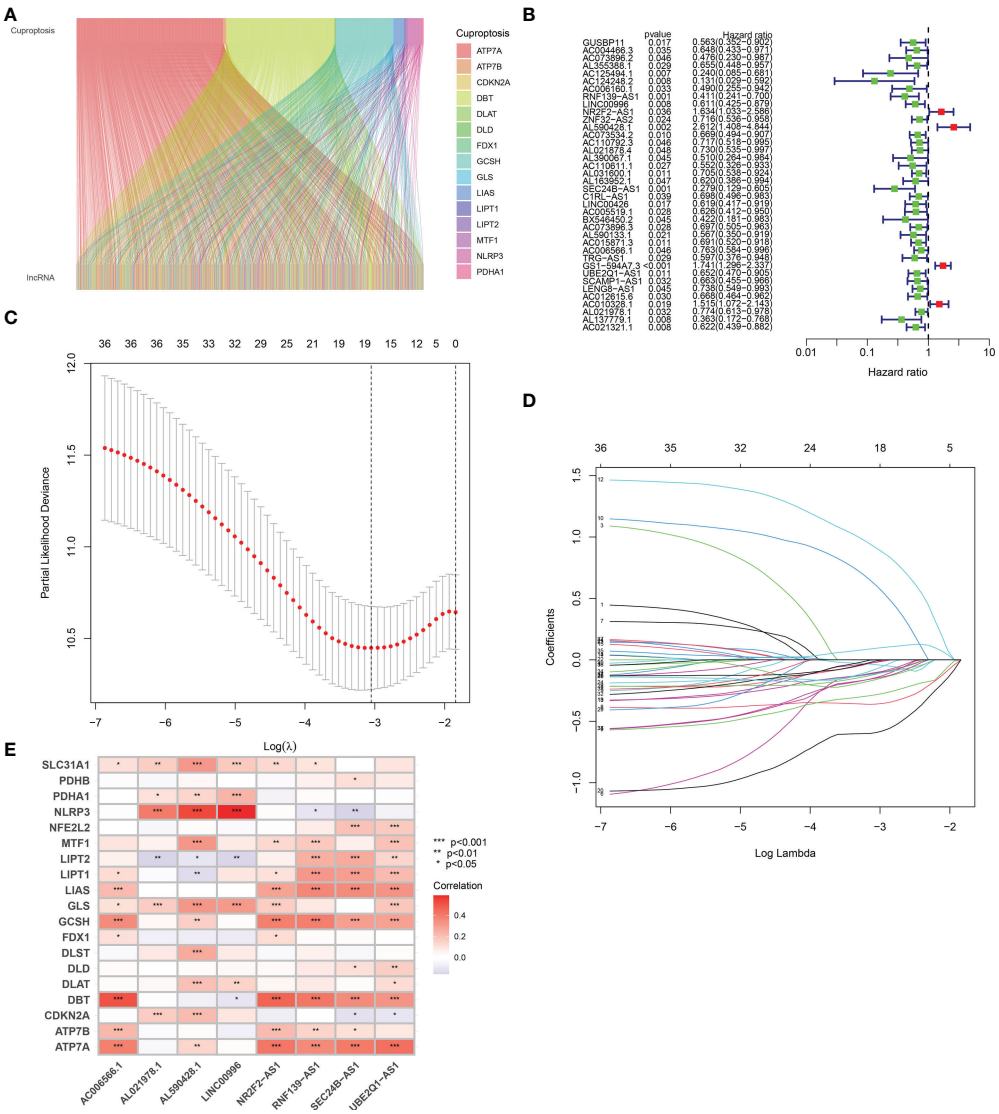

FIGURE 2
Defining the cuproptosis-related lncRNAs with prognostic significance in BLCA. **(A)** A total of 961 cuproptosis-related lncRNAs were identified in BLCA. **(B)** The forest plot revealed cuproptosis-related lncRNAs with significant prognostic value. **(C)** The 10-fold cross-validation of variable selection in the least absolute shrinkage and selection operator (LASSO) algorithm. **(D)** Correlation of lncRNAs with cuproptosis-related genes in prognostic signature. **(E)** The correlation between prognostic signature and cuproptosis-related genes. *$p < 0.05$, **$p < 0.01$, and ***$p < 0.001$.

prognostic signature in different clinical stages. The result also suggested that BLCA patients with a high risk score had a poor OS in both stage I–II (Figure 5C, $p = 0.014$) and stage III–IV groups (Figure 5D, $p < 0.001$).

The principal components analysis and biological pathways analyses

In order to identify whether the cuproptosis-related lncRNA prognostic signature could cluster BLCA cases into the high- and low-risk groups, PCA was performed. Interestingly, comparing the gene module (Figure 6A), cuproptosis-related gene module (Figure 6B), cuproptosis-related lncRNA module (Figure 6C), and cuproptosis-related lncRNAs prognostic module (Figure 6D) could more clearly cluster BLCA cases into the high- and low-risk groups. In order to clarify the difference between the high- and low-risk groups, we also performed GO and KEGG pathway analysis using the differentially expressed genes between these two groups. GO analysis revealed that these cuproptosis-associated lncRNAs were mainly linked to epidermis development, omega-hydroxylase P450 pathway, T-

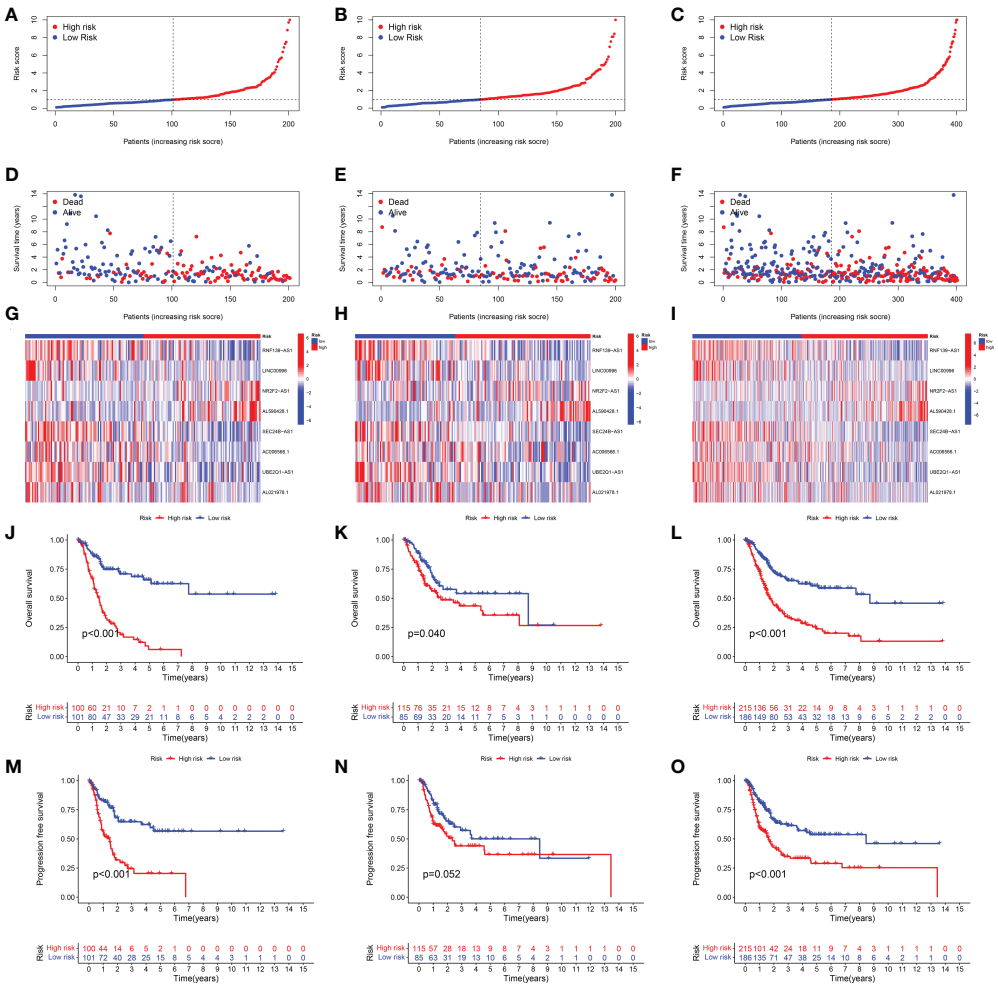

FIGURE 3
Development of the cuproptosis-related lncRNA prognostic signature in BLCA. The risk score **(A–C)**, survival status **(D–F)**, and gene expression **(G–I)** of prognostic signature in the training set, test set, and complete set. Kaplan–Meier survival curves of overall survival (OS, **J–L**) and progression-free survival (PFS, **M–O**) in the high- and low-risk groups of BLCA in the train set, test set, and complete set.

cell receptor complex, aromatase activity, and enzyme inhibitor activity (Figures 7A, B). Moreover, KEGG pathway analysis suggested the involvement in cholesterol metabolism, complement and coagulation cascades, PPAR signaling pathway, and Wnt signaling pathway (Figures 7C, D).

Immune infiltration

We further surveyed the difference between the high- and low-risk groups in common immune-related activities. However, no significant difference was obtained between the high- and low-risk groups in common immune-related activities (Figure 8A). To explore the relationship between the immune system and the risk assessment model, recognized methods, including XCELL, TIMER, QUANTISEQ, MCPCOUNTER, EPIC, CIBERSORT-ABS, and CIBERSORT, were used. As a result, the lollipop chart (Figure 8B) shows that patients in the high-risk group are positively correlated with tumor-infiltrating immune cells (such as cancer-related fibroblasts, common myeloid progenitor cells, endothelial cells, hematopoietic stem cells, M0 macrophages, M2 macrophages, stroma score, and uncharacterized cells), and they are negatively correlated with memory B cells, plasma B cells, B cells, class-switched memory B cells, CD4+ central memory T cells, CD4+ memory activated T cells, CD4+ memory T cells, CD4+ naïve T cells, CD4+ T cells, follicular helper T cells, regulator T cells (Tregs), and T cells by Spearman correlation analysis (see Supplement 1 for details).

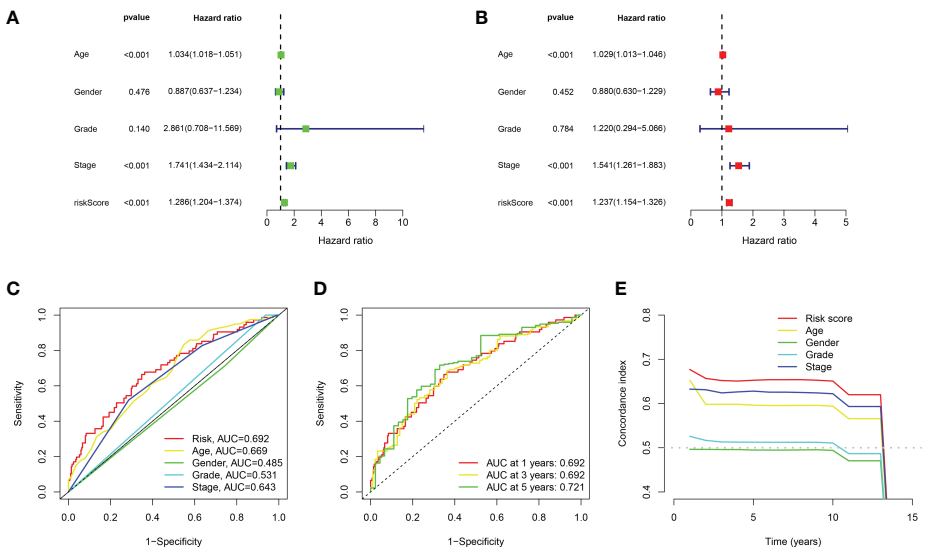

FIGURE 4
Evaluation about the accuracy of the cuproptosis-related lncRNA prognostic signature in BLCA. **(A, B)** Univariate Cox regression analysis considering risk score and clinical characteristics. **(C)** ROC curve considering risk score and clinical characteristics. **(D)** ROC curve of 1-year, 3-year, and 5-year overall survival. **(E)** C-index curve of the prognostic signature.

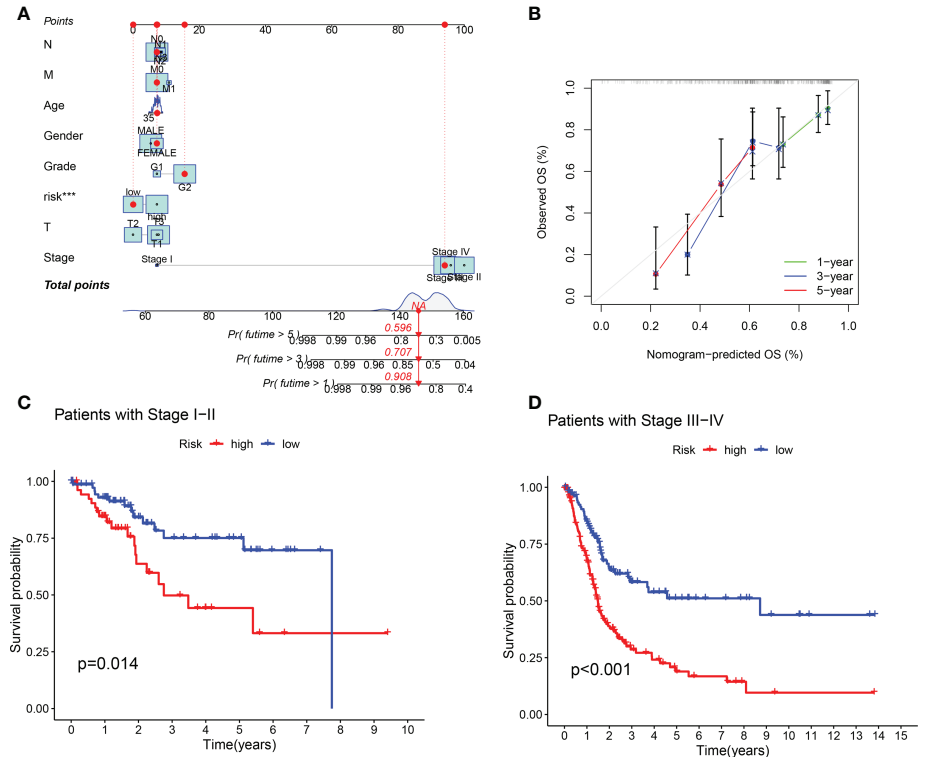

FIGURE 5
Construction of predictive nomogram and survival curve based on subgroup analysis. **(A, B)** A nomogram considering clinicopathological variables and risk scores predicts overall survival in BLCA. **(C, D)** Survival curve of the high-/low-risk group in different stages of BLCA patients.

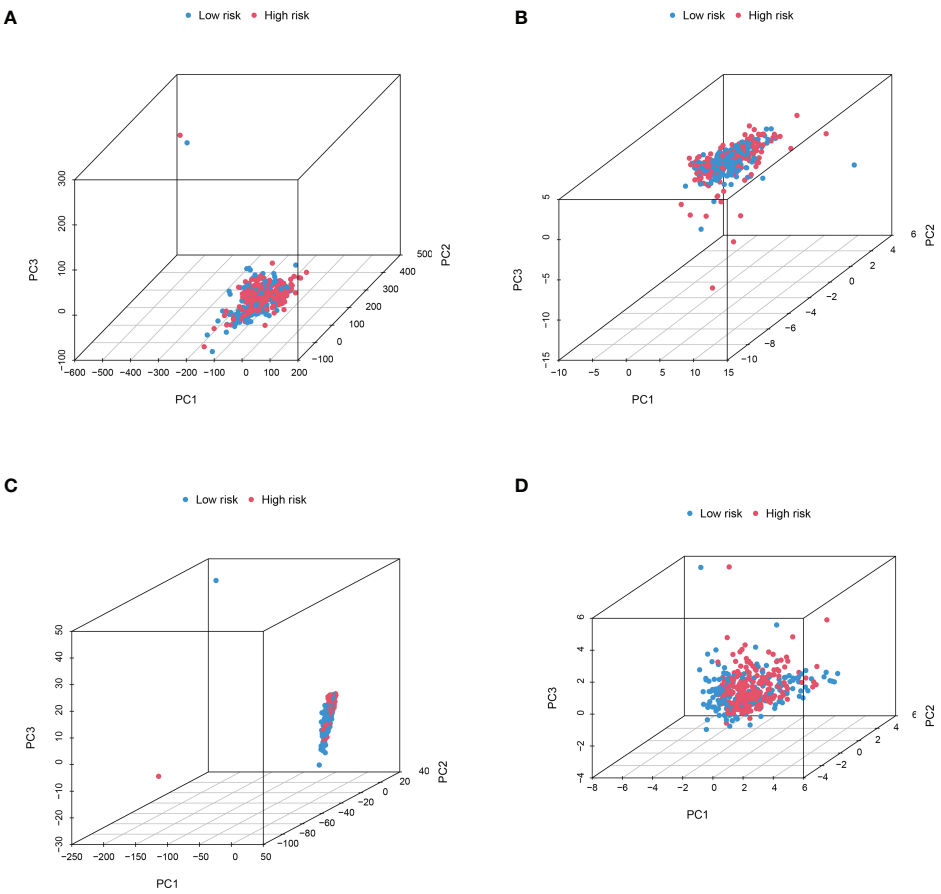

FIGURE 6
PCA considering the different gene profiles of BLCA patients. Comparing the gene module **(A)**, cuproptosis-related gene module **(B)**, cuproptosis-related lncRNA module **(C)**, and cuproptosis-related lncRNA prognostic module **(D)** could more clearly cluster BLCA cases into high- and low-risk groups.

TMB, TIDE, and drug sensitivity

We also explored the difference between the high- and low-risk groups in TMB, TIDE, and drug sensitivity. For TMB analysis, we found that the 15 most highly mutated genes were TP53, TTN, KMT2D, MUC16, ARID1A, KDM6A, PIK3CA, SYNE1, KMT2C, RYR2, HMCN1, RB1, FAT4, MACF1, and EP300 in BLCA. As shown in Figures 8C, D, the mutation rate of these genes was higher in the high-risk group, including TP53, ARID1A, KMT2C, RYR2, and RB1. On the contrary, the mutation rate of the remaining genes was higher in the low-risk group, including TTN, KMT2D, MUC16, KDM6A, PIK3CA, SYNE1, HMCN1, FAT4, MACF1, and EP300. Interestingly, BLCA patients with a low risk score had a higher TMB level (Figure 8E, $p = 0.00045$). Further analysis suggested that BLCA patients with a low TMB and a high risk score had a poor OS rate (Figures 8F, G, $p < 0.001$). As shown in Figure 8H, BLCA patients with a high risk score had a higher TIDE score than those with a low risk score ($p < 0.01$). Further analysis also revealed that BLCA patients with a high risk score had a higher IC_{50} value of many therapeutic drugs than those with a low risk score (Figures 9A–Y). These results suggested that BLCA patients with a high risk score may be more likely to be resistant to chemotherapy and immunotherapy.

Discussion

BLCA is the second most frequent genitourinary cancer, with a growing incidence worldwide (29). The symptoms of BLCA were similar to urinary infection, thus delaying timely diagnosis (30). It is estimated that 1/4 of the initially diagnosed cases was muscle-invasive BLCA (31). Moreover, BLCA is characterized by high recurrence rate and poor prognosis. The prognosis of patients with muscle-invasive BLCA was less favorable, and the 5-year survival rate was less than 50% (6). Thus, there is an urgent need to identify the reliably prognostic biomarkers and novel therapy targets of BLCA.

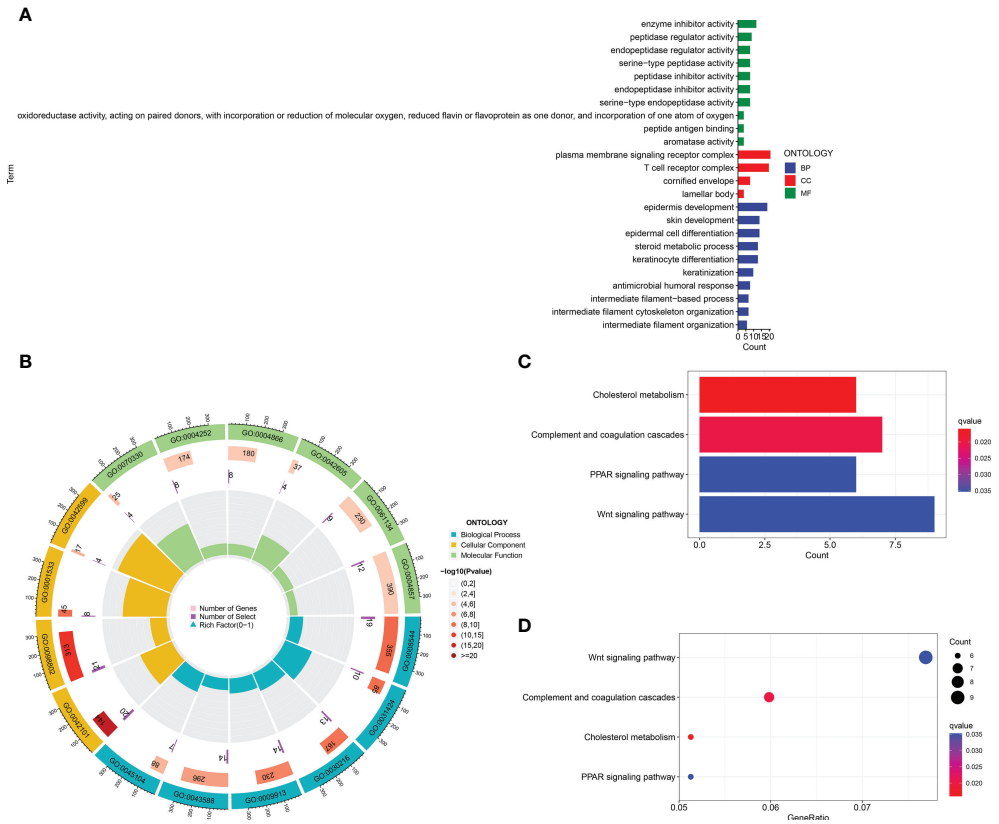

FIGURE 7
GO and KEGG analysis. The enrichment items in GO **(A, B)** and KEGG pathway **(C, D)** analysis.

Metal ions are essential micronutrients in mammals. However, insufficient or excessive metal ions do harm to health and lead to cell death (8). A recent study performed by Tsvetkov et al. reported that excess copper contributes to the aggregation of lipoylated dihydrolipoamide S-acetyltransferase intracellularly, leading to a novel of mitochondrial cell death called "cuproptosis" (8, 17). Increasing lines of evidence had constructed a cuproptosis-related signature for the prognosis and immune response of certain types of cancer (32–34).

Accumulating studies have reported the significant role of lncRNAs in the development and progression of BLCA. lncRNA-RMRP could accelerate the proliferation, migration, and invasion of BLCA cells (35). By regulating E2F1, lncRNA-SLC16A1-AS1 could promote metabolic reprogramming in BLCA (36). Moreover, lncRNA TUC338 was considered as a diagnostic biomarker for BLCA (37). Another meta-analysis revealed that lncRNAs could serve as a diagnostic and prognostic biomarker in BLCA (38). However, the prognosis value of cuproptosis-related lncRNAs and their correlation with immune landscape in BLCA had not been fully clarified.

We first constructed a cuproptosis-related lncRNA prognostic signature for BLCA including eight lncRNAs (RNF139-AS1, LINC00996, NR2F2-AS1, AL590428.1, SEC24B-AS1, AC006566.1, UBE2Q1-AS1, and AL021978.1). Further analysis revealed that this prognostic signature not only had higher diagnostic efficiency compared to other clinical features but also had a good performance in predicting the 1-year, 3-year, and 5-year OS in BLCA. Actually, many studies had reported that cuproptosis-related lncRNA signature could serve as a prognostic biomarker in many types of cancer. Liu et al. constructed cuproptosis-related lncRNAs as biomarkers of prognosis and the immune microenvironment in squamous cell carcinoma (39). Another cuproptosis-related lncRNA signature could guide the prognosis and immune microenvironment in osteosarcoma (40). Yun also developed a cuproptosis-related prognostic signature in uterine corpus endometrial carcinoma (41). In colon adenocarcinoma, the cuproptosis-related lncRNA signature could provide insights into the accurate prediction of prognosis (32).

GO and KEGG pathway analysis revealed that these cuproptosis-associated lncRNAs were mainly linked to epidermis development, omega-hydroxylase P450 pathway, T-cell receptor complex, aromatase activity and enzyme inhibitor activity, cholesterol metabolism, complement and coagulation

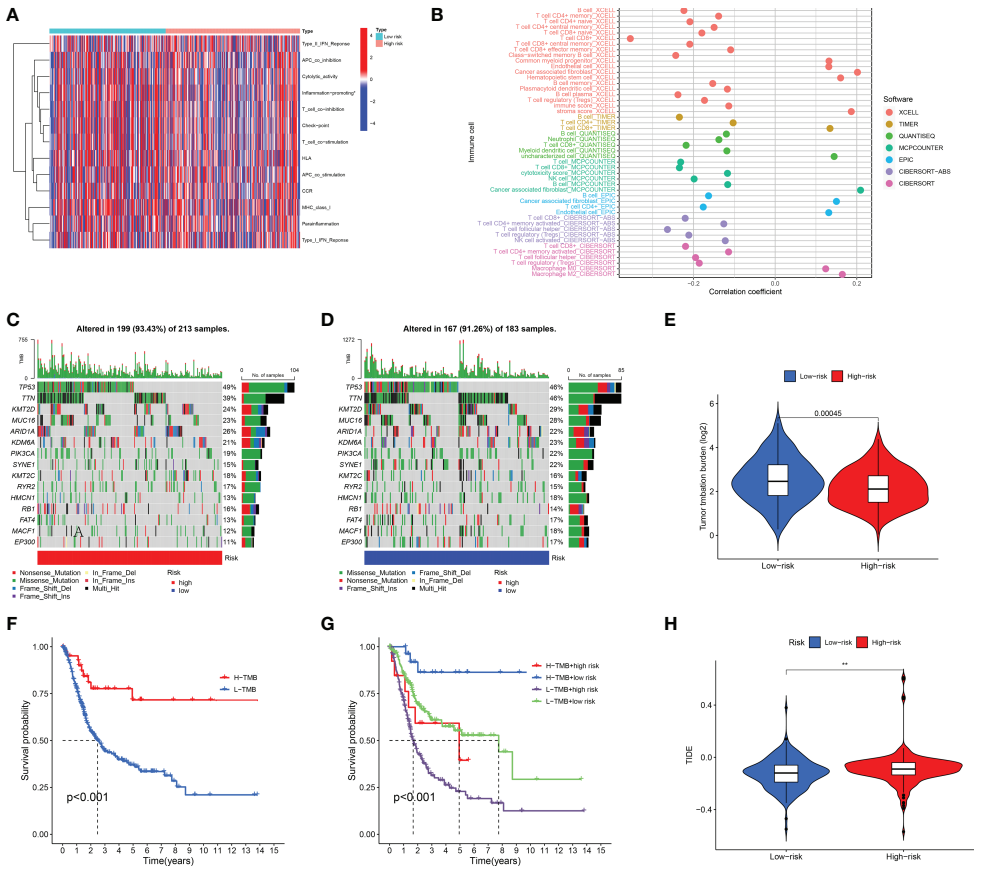

FIGURE 8
Immune-related activity, TMB, and TIDE analysis. The difference in immune-related activities **(A)** and tumor-infiltrating immune cells **(B)**. The difference in somatic mutation characteristics **(C, D)** between the high- and low-risk groups. **(E)** TMB between the low-risk and high-risk groups of BLCA patients. **(F, G)** Survival curve in the different groups of BLCA patients. **(H)** TIDE scores between the low-risk and high-risk groups of BLCA patients. **(F)** shows that among bladder cancer patients, the high tumor mutation burden group (H-TMB) was associated with a better prognosis. **p < 0.01.

cascades, PPAR signaling pathway, and Wnt signaling pathway. Among these signaling pathways, PPAR signaling exerts pleiotropic functions in cancer (42). Moreover, PPARγ inhibition was involved in the regulation of cell cycle, and proliferation and motility of BLCA (43). Moreover, Wnt signaling pathway was also associated with tumor cell invasion and metastasis in BLCA (44). The tumor microenvironment of BLCA was also associated with Wnt signaling pathway (45). Thus, cuproptosis-associated lncRNAs might regulate biological processes in BLCA *via* these pathways. Further study should be performed to verify these results. As mentioned above, our novel cuproptosis-related lncRNA signatures also predict the relationship between tumor-infiltrating immune cells and BLCA. These lncRNAs also play an important role in the immunity of other diseases. For example, previous studies have shown that LNC00996 is overexpressed in lung adenocarcinoma and squamous cell carcinoma, and is closely related to the immune system (46). In addition, AL590428.1 was downregulated in human pterygium fibroblasts, which is closely related to cell cycle and apoptosis (47).

As is known, the TIDE algorithm was performed to assess the clinical response to immune checkpoint inhibitor (ICI) treatment. A higher TIDE score indicates a greater likelihood of immune escape, meaning that patients treated with ICI have a limited response and a shorter survival time (11). Thus, another vital finding of our study was that BLCA patients with a high risk score had a higher TIDE score compared with patients with a low risk score. For TMB analysis, we found the 15 most highly mutated genes in BLCA. Among them, the mutation rate of TP53 was higher in the high-risk group. As we know, the transcription factor p53 is a key tumor suppressor that is inactivated in almost all cancers due to point mutations in the TP53 gene or overexpression of its negative regulator. The p53 protein is known as the “cellular gatekeeper” because of its role in promoting DNA repair, cell cycle arrest, or apoptosis in response to DNA damage (48). Moreover, IC_{50} is an

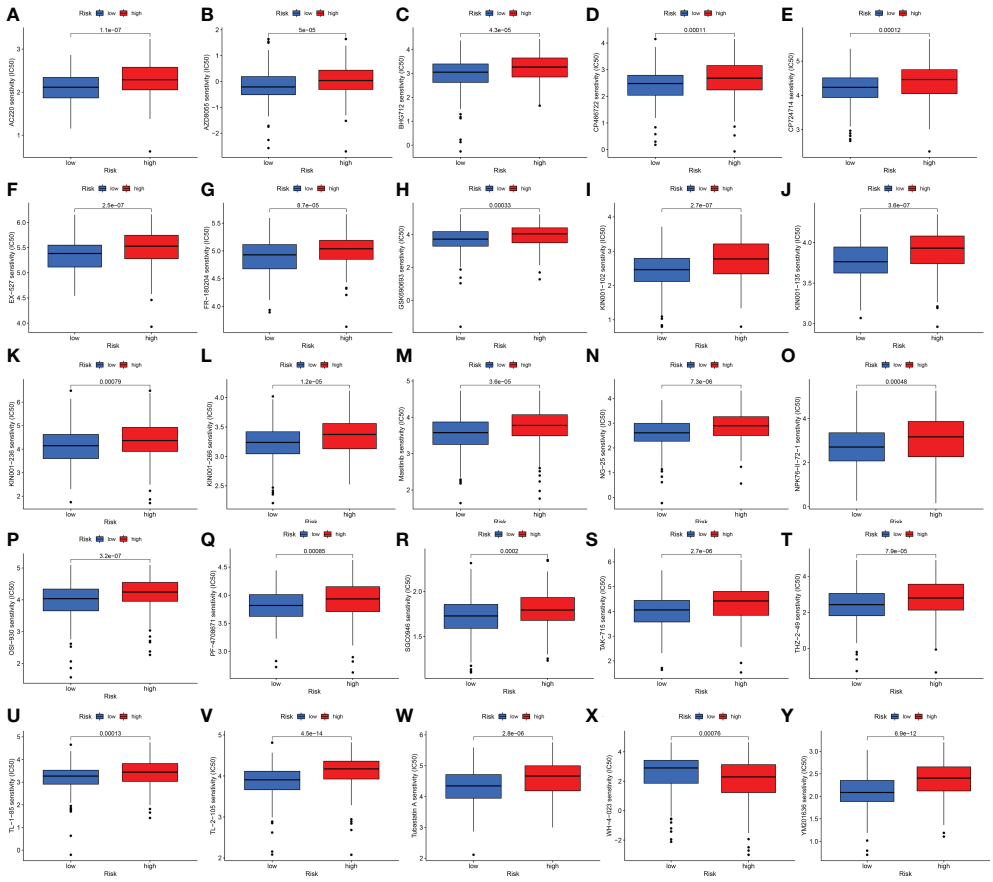

FIGURE 9
Drug sensitivity analysis. **(A–Y)** BLCA patients with a high risk score had a higher IC_{50} value of many therapeutic drugs compared with patients with a low risk score.

important index for evaluating drug efficacy or sample response to treatment, and cancer patients with a higher IC_{50} value had a greater likelihood of drug resistance (49). In our study, BLCA patients with a high risk score had a higher IC_{50} value of many therapeutic drugs compared with patients with a low risk score. The above drugs contain AC220, AZD8055, BHG712, CP466722, CP724714, EX-527, FR-180204, GSJ690693, KIN001-102, KIN001-135, KIN001-236, KIN001-266, Masitinib, NG-25, NPK76-II-72-1, OSI-930, PF-4708671, SGC0946, TAK-715, THZ-2-49, TL-1-85, TL-2-105, Tubastatin A, WH-4-023, and YM201636. Among these drugs, as a novel receptor tyrosine kinase inhibitor, Masitinib (also known as AB1010) has been shown to have inhibitory activity and increase apoptosis in bladder TCC cells, and is positively correlated with PDGFRα and c-Kit receptor expression levels (50). Moreover, as a special HDAC6 inhibitor, Tubastatin A (TST) can affect cell growth and promote structural modifications in cancer cells and parasites, which are potential anti-*Toxoplasma gondii* chemotherapeutics (51, 52). Urdician et al. found that TST could enhance temozolomide–induced apoptosis and change the malignant phenotype of glioblastoma cells (53). Thus, our results suggested that BLCA patients with a high risk score may be more likely to be resistant to chemotherapy and immunotherapy, which may be used to guide the treatment of patients with BLCA.

The current study had several limitations that should be acknowledged. First of all, the data in this study come from a single source. Due to the deviation and limitation of commercial microarray, we cannot get verification from the GEO and ICGC database. Secondly, we did not verify the above lncRNAs, including their expression and mechanism in BLCA. Finally, the immune cell bubble map shows the results of immune infiltration in multiple platforms, which can be considered external validation in a sense and lacks rigor. Therefore, in the future, we should not only verify the accuracy and practicality of the above lncRNA signature by collecting a large number of clinical data, but also further explore the mechanism of these lncRNAs in BLCA.

Conclusion

In conclusion, this novel cuproptosis-related lncRNA signature helps us not only to predict the prognosis of BLCA, but also to understand the immune landscape and drug sensitivity of BLCA. Further investigation is still needed to validate these findings.

Data availability statement

Publicly available datasets were analyzed in this study. This data can be found here: the TCGA-BLCA (https://portal.gdc.cancer.gov/).

Author contributions

JQ and YB conducted the formal analysis and wrote the original draft. FL and QZ performed project administration. JQ provided software and conducted data curation. YB, FL and QZ contributed to writing, reviewing, and editing the article. All authors contributed to the article and approved the submitted version.

Funding

This study was supported by the General Project Funds from the Health Department of Zhejiang Province (Grant no. 2021439557), General Project Funds from the Health Department of Zhejiang Province (Grant no. 2022496245), and Project Funds of Zhejiang Provincial Science and Technology Department (Grant no. LY18H160040).

Conflict of interest

The authors declare that the research was conducted in the absence of any commercial or financial relationships that could be construed as a potential conflict of interest.

Publisher's note

All claims expressed in this article are solely those of the authors and do not necessarily represent those of their affiliated organizations, or those of the publisher, the editors and the reviewers. Any product that may be evaluated in this article, or claim that may be made by its manufacturer, is not guaranteed or endorsed by the publisher.

Supplementary material

The Supplementary Material for this article can be found online at: https://www.frontiersin.org/articles/10.3389/fimmu.2022.1027449/full#supplementary-material

References

1. Patel VG, Oh WK, Galsky MD. Treatment of muscle-invasive and advanced bladder cancer in 2020. *CA Cancer J Clin* (2020) 70:404–23. doi: 10.3322/caac.21631

2. Richters A, Aben KKH, Kiemeney L. The global burden of urinary bladder cancer: an update. *World J Urol* (2020) 38:1895–904. doi: 10.1007/s00345-019-02984-4

3. Lenis AT, Lec PM, Chamie K, MSHS MD. Bladder cancer: A review. *Jama* (2020) 324:1980–91. doi: 10.1001/jama.2020.17598

4. Kimura T, Ishikawa H, Kojima T, Kandori S, Kawahara T, Sekino Y, et al. Bladder preservation therapy for muscle invasive bladder cancer: the past, present and future. *Jpn J Clin Oncol* (2020) 50:1097–107. doi: 10.1093/jjco/hyaa155

5. Vasekar M, Degraff D, Joshi M. Immunotherapy in bladder cancer. *Curr Mol Pharmacol* (2016) 9:242–51. doi: 10.2174/1874467208666150716120945

6. Cao R, Yuan L, Ma B, Wang G, Qui W, Tian Y. An EMT-related gene signature for the prognosis of human bladder cancer. *J Cell Mol Med* (2020) 24:605–17. doi: 10.1111/jcmm.14767

7. Knowles MA, Hurst CD. Molecular biology of bladder cancer: new insights into pathogenesis and clinical diversity. *Nat Rev Cancer* (2015) 15:25–41. doi: 10.1038/nrc3817

8. Tang D, Chen X, Kroemer G. Cuproptosis: A copper-triggered modality of mitochondrial cell death. *Cell Res* (2022) 32:417–8. doi: 10.1038/s41422-022-00653-7

9. Wang Y, Zhang L, Zhou F. Cuproptosis: a new form of programmed cell death. *Cell Mol Immunol* (2022) 19:867–8. doi: 10.1038/s41423-022-00866-1

10. Bian Z, Fan R, Xie L. A novel cuproptosis-related prognostic gene signature and validation of differential expression in clear cell renal cell carcinoma. *Genes* (2022) 13:851. doi: 10.3390/genes13050851

11. Xu S, Liu D, Chang T, Wen X, Ma S, Sun G, et al. Cuproptosis-associated lncRNA establishes new prognostic profile and predicts immunotherapy response in clear cell renal cell carcinoma. *Front Genet* (2022) 13:938259. doi: 10.3389/fgene.2022.938259

12. Zhang G, Sun J, Zhang X. A novel cuproptosis-related LncRNA signature to predict prognosis in hepatocellular carcinoma. *Sci Rep* (2022) 12:11325. doi: 10.1038/s41598-022-15251-1

13. Lv H, Liu X, Zeng X, Liu Y, Zhang C, Zhang Q, et al. Comprehensive analysis of cuproptosis-related genes in immune infiltration and prognosis in melanoma. *Front Pharmacol* (2022) 13:930041. doi: 10.3389/fphar.2022.930041

14. Xing C, Sun SG, Yue ZQ, Bai F. Role of lncRNA LUCAT1 in cancer. *BioMed Pharmacother* (2021) 134:111158. doi: 10.1016/j.biopha.2020.111158

15. Li Z, Li Y, Zhong W, Huang P. m6A-related lncRNA to develop prognostic signature and predict the immune landscape in bladder cancer. *J Oncol* (2021) 2021:7488188. doi: 10.1155/2021/7488188

16. Chen C, Luo Y, He W, Zhao Y, Kong Y, Liu H, et al. Exosomal long noncoding RNA LNMAT2 promotes lymphatic metastasis in bladder cancer. *J Clin Invest* (2020) 130:404–21. doi: 10.1172/jci130892

17. Tsvetkov P, Coy S, Petrova B, Dreishpoon M, Verma A, Abdusamad M, et al. Copper induces cell death by targeting lipoylated TCA cycle proteins. *Science* (2022) 375:1254–61. doi: 10.1126/science.abf0529

18. Tao X, Wan X, Wu D, Song Y. A tandem activation of NLRP3 inflammasome induced by copper oxide nanoparticles and dissolved copper ion in J774A.1 macrophage. *J Hazard Mater* (2021) 411:125134. doi: 10.1016/j.jhazmat.2021.125134

19. Tavera-Montañez C, Hainer SJ, Cangussu D, Gordon SJV, Xiao Y, Reyes-Gutierrez P, et al. The classic metal-sensing transcription factor MTF1 promotes myogenesis in response to copper. *FASEB J* (2019) 33:14556–74. doi: 10.1096/fj.201901606R

20. Yin F, Nian M, Wang N, Wu H, Wu H, Zhao W, et al. Protective mechanism of gandou decoction in a copper-laden hepatolenticular degeneration model: *In vitro* pharmacology and cell metabolomics. *Front Pharmacol* (2022) 13:848897. doi: 10.3389/fphar.2022.848897

21. Lelièvre P, Sancey L, Coll JL, Deniaud A, Busser B. The multifaceted roles of copper in cancer: A trace metal element with dysregulated metabolism, but also a target or a bullet for therapy. *Cancers (Basel)* (2020) 12:3954. doi: 10.3390/cancers12123594

22. Aran D, Hu Z, Butte AJ. xCell: digitally portraying the tissue cellular heterogeneity landscape. *Genome Biol* (2017) 18:220. doi: 10.1186/s13059-017-1349-1

23. Li T, Fan J, Wang B, Traugh N, Chen Q, Liu JS, et al. TIMER: A web server for comprehensive analysis of tumor-infiltrating immune cells. *Cancer Res* (2017) 77:e108–10. doi: 10.1158/0008-5472.Can-17-0307

24. Finotello F, Mayer C, Plattner C, Laschober G, Rieder D, Hackl H, et al. Molecular and pharmacological modulators of the tumor immune contexture revealed by deconvolution of RNA-seq data. *Genome Med* (2019) 11:34. doi: 10.1186/s13073-019-0638-6

25. Becht E, Giraldo NA, Lacroix L, Buttard B, Elarouci N, Petitprez F, et al. Estimating the population abundance of tissue-infiltrating immune and stromal cell populations using gene expression. *Genome Biol* (2016) 17:218. doi: 10.1186/s13059-016-1070-5

26. Racle J, Gfeller D. EPIC: A tool to estimate the proportions of different cell types from bulk gene expression data. *Methods Mol Biol* (2020) 2120:233–48. doi: 10.1007/978-1-0716-0327-7_17

27. Chen B, Khodadoust MS, Liu CL, Newman AM, Alizadeh AA. Profiling tumor infiltrating immune cells with CIBERSORT. *Methods Mol Biol* (2018) 1711:243–59. doi: 10.1007/978-1-4939-7493-1_12

28. Tamminga M, Hiltermann TJN, Schuuring E, Timens W, Fehrmann RS, Groen HJ, et al. Immune microenvironment composition in non-small cell lung cancer and its association with survival. *Clin Transl Immunol* (2020) 9:e1142. doi: 10.1002/cti2.1142

29. Bhanvadia SK. Bladder cancer survivorship. *Curr Urol Rep* (2018) 19:111. doi: 10.1007/s11934-018-0860-6

30. Farling KB. Bladder cancer: Risk factors, diagnosis, and management. *Nurse Pract* (2017) 42:26–33. doi: 10.1097/01.NPR.0000512251.61454.5c

31. Seidl C. Targets for therapy of bladder cancer. *Semin Nucl Med* (2020) 50:162–70. doi: 10.1053/j.semnuclmed.2020.02.006

32. Xu M, Mu J, Wang J, Zhou Q, Wang J. Construction and validation of a cuproptosis-related lncRNA signature as a novel and robust prognostic model for colon adenocarcinoma. *Front Oncol* (2022) 12:961213. doi: 10.3389/fonc.2022.961213

33. Yun Y, Wang Y, Yang E, Jing X. Cuproptosis-related gene - SLC31A1, FDX1 and ATP7B - polymorphisms are associated with risk of lung cancer. *Pharmgenomics Pers Med* (2022) 15:733–42. doi: 10.2147/pgpm.S372824

34. Zhang C, Zeng Y, Guo X, Shen H, Zhang J, Wang K, et al. Pan-cancer analyses confirmed the cuproptosis-related gene FDX1 as an immunotherapy predictor and prognostic biomarker. *Front Genet* (2022) 13:923737. doi: 10.3389/fgene.2022.923737

35. Cao HL, Liu ZJ, Huang PL, Yue YL, Xi JN. lncRNA-RMRP promotes proliferation, migration and invasion of bladder cancer *via* miR-206. *Eur Rev Med Pharmacol Sci* (2019) 23:1012–21. doi: 10.26355/eurrev_201902_16988

36. Logotheti S, Marquardt S, Gupta SK, Richter C, Edelhäuser BAH, Engelmann D, et al. LncRNA-SLC16A1-AS1 induces metabolic reprogramming during bladder cancer progression as target and co-activator of E2F1. *Theranostics* (2020) 10:9620–43. doi: 10.7150/thno.44176

37. Li G, Zhang Y, Mao J, Hu P, Chen Q, Ding W, et al. lncRNA TUC338 is a potential diagnostic biomarker for bladder cancer. *J Cell Biochem* (2019) 120:18014–9. doi: 10.1002/jcb.29104

38. Quan J, Pan X, Zhao L, Li Z, Dai K, Yan F, et al. LncRNA as a diagnostic and prognostic biomarker in bladder cancer: a systematic review and meta-analysis. *Onco Targets Ther* (2018) 11:6415–24. doi: 10.2147/ott.S167853

39. Yang L, Yu J, Tao L, Huang H, Gao Y, Yao J, et al. Cuproptosis-related lncRNAs are biomarkers of prognosis and immune microenvironment in head and neck squamous cell carcinoma. *Front Genet* (2022) 13:947551. doi: 10.3389/fgene.2022.947551

40. Yang M, Zheng H, Xu K, Yuan Q, Aihaiti Y, Cai Y, et al. A novel signature to guide osteosarcoma prognosis and immune microenvironment: Cuproptosis-related lncRNA. *Front Immunol* (2022) 13:919231. doi: 10.3389/fimmu.2022.919231

41. Chen Y. Identification and validation of cuproptosis-related prognostic signature and associated regulatory axis in uterine corpus endometrial carcinoma. *Front Genet* (2022) 13:912037. doi: 10.3389/fgene.2022.912037

42. Chang WH, Lai AG. The pan-cancer mutational landscape of the PPAR pathway reveals universal patterns of dysregulated metabolism and interactions with tumor immunity and hypoxia. *Ann N Y Acad Sci* (2019) 1448:65–82. doi: 10.1111/nyas.14170

43. Cheng S, Qian K, Wang Y, Wang G, Liu X, Xiao Y, et al. PPARγ inhibition regulates the cell cycle, proliferation and motility of bladder cancer cells. *J Cell Mol Med* (2019) 23:3724–36. doi: 10.1111/jcmm.14280

44. Zhang M, Du H, Wang L, Yue Y, Zhang P, Huang Z, et al. Thymoquinone suppresses invasion and metastasis in bladder cancer cells by reversing EMT through the wnt/β-catenin signaling pathway. *Chem Biol Interact* (2020) 320:109022. doi: 10.1016/j.cbi.2020.109022

45. Wu G, Weng W, Xia P, Yan S, Zhong C, Xie L, et al. Wnt signalling pathway in bladder cancer. *Cell Signalling* (2021) 79:109886. doi: 10.1016/j.cellsig.2020.109886

46. Yan T, Ma G, Wang K, Liu W, Zhong W, Du J, et al. The immune heterogeneity between pulmonary adenocarcinoma and squamous cell carcinoma: A comprehensive analysis based on lncRNA model. *Front Immunol* (2021) 12:547333. doi: 10.3389/fimmu.2021.547333

47. Zhao D, Zhao H, He Y, Yang Y, Du Y, Zhang M, et al. The inhibitive effects of proteasome inhibitor MG-132 on pterygium fibroblasts *in vitro* and the potential key regulators involved. *Life Sci* (2021) 270:119088. doi: 10.1016/j.lfs.2021.119088

48. Chasov V, Mirgayazova R, Zmievskaya E, Khadiullina R, Valiullina A, Clarke Stephenson J, et al. Key players in the mutant p53 team: Small molecules, gene editing, immunotherapy. *Front Oncol* (2020) 10:1460. doi: 10.3389/fonc.2020.01460

49. Geeleher P, Cox NJ, Huang RS. Clinical drug response can be predicted using baseline gene expression levels and *in vitro* drug sensitivity in cell lines. *Genome Biol* (2014) 15:R47. doi: 10.1186/gb-2014-15-3-r47

50. Bourn J, Cekanova M. Cyclooxygenase inhibitors potentiate receptor tyrosine kinase therapies in bladder cancer cells in vitro. *Drug Des Devel Ther* (2018) 12:1727–42. doi: 10.2147/dddt.S158518

51. de Oliveira Santos J, Zuma AA, de Souza W, Motta MCM, Tubastatin A, Tubastatin A. A deacetylase inhibitor, as a tool to study the division, cell cycle and microtubule cytoskeleton of trypanosomatids. *Eur J Protistol* (2021) 80:125821. doi: 10.1016/j.ejop.2021.125821

52. Araujo-Silva CA, De Souza W, Martins-Duarte ES, Vommaro RC. HDAC inhibitors tubastatin a and SAHA affect parasite cell division and are potential anti-toxoplasma gondii chemotherapeutics. *Int J Parasitol Drugs Drug Resist* (2021) 15:25–35. doi: 10.1016/j.ijpddr.2020.12.003

53. Urdiciain A, Erausquin E, Meléndez B, Rey JA, Idoate MA, Castresana JS. Tubastatin a, an inhibitor of HDAC6, enhances temozolomide–induced apoptosis and reverses the malignant phenotype of glioblastoma cells. *Int J Oncol* (2019) 54:1797–808. doi: 10.3892/ijo.2019.4739